

## Accepted Article

**Title:** Synthesis and characterization of a ruthenium(II) complex for the development of supramolecular photocatalysts containing multidentate coordination spheres

**Authors:** Fabian L. Huber, Djawed Nauroozi, Mengele Alexander, and Sven Rau

This manuscript has been accepted after peer review and appears as an Accepted Article online prior to editing, proofing, and formal publication of the final Version of Record (VoR). This work is currently citable by using the Digital Object Identifier (DOI) given below. The VoR will be published online in Early View as soon as possible and may be different to this Accepted Article as a result of editing. Readers should obtain the VoR from the journal website shown below when it is published to ensure accuracy of information. The authors are responsible for the content of this Accepted Article.

**To be cited as:** *Eur. J. Inorg. Chem.* 10.1002/ejic.201700565

**Link to VoR:** <http://dx.doi.org/10.1002/ejic.201700565>

# Synthesis and characterization of a ruthenium(II) complex for the development of supramolecular photocatalysts containing multidentate coordination spheres

Fabian L. Huber,<sup>[a]</sup> Djawed Nauroozi,<sup>[a]</sup> Alexander K. Mengele,<sup>[a]</sup> and Sven Rau<sup>\*[a]</sup>

**Abstract:** The synthesis of the new Ru<sup>II</sup> bis-heteroleptic complex [(tbbpy)<sub>2</sub>Ru(dptpphz)](PF<sub>6</sub>)<sub>2</sub> (**7**), that exhibits a tetradentate coordination sphere for a second metal centre, and its characterization are presented. The complex shows a similar photostability and redox properties regarding the first ligand centred reductions compared to its tpphz analogue. Concentration dependent NMR investigations were performed and a dimerization constant ( $K_D = 83 \pm 5$ ) could be calculated, which was significantly lower compared to other tpphz systems. Photophysical investigations reveal a stabilizing effect of the two electron withdrawing 2-pyridyl substituents on  $\pi$ - $\pi^*$  transition of the phenazine sphere. The typical H<sub>2</sub>O induced light switch effects have also been observed. To further highlight the potential of the tetradentate coordination site, the Zn<sup>II</sup> adduct of **7** was prepared and preliminary studied.

## Introduction

Since PMDs (photochemical molecular devices) do not rely on diffusion controlled electron transfer processes, contrary to intermolecular systems, multiple supramolecular photocatalysts for the light driven reduction of water and CO<sub>2</sub> have been developed.<sup>[1-5]</sup> Especially systems based on the tpphz, bridging ligand (tetrapyrido[3,2-a:2',3'-c:3'',2''-h:2''',3'''-j]phenazine), which was first introduced by Bolger et al.,<sup>[6,7]</sup> are well investigated.<sup>[4,8,9]</sup> In supramolecular systems it enables the desired vectorial electron transfer from the photosensitizer towards the catalytic centre on a sub-nanosecond scale upon light absorption. Spectroscopic studies relying on ultrafast time resolved absorption and resonance Raman spectroscopy were carried out on mono- and dinuclear ruthenium and osmium oligopyridophenazine complexes, shining light on the mechanism of excited state electron transfers.<sup>[10-13]</sup> Multiple efforts with the aim of tuning the properties and enhancing the stability of tpphz complexes have been taken by synthesising and studying various substituted tpphz derivatives.<sup>[14-18]</sup> One approach aimed to stabilize the catalytic centre by introducing electron donating *p*-anisyl substituents in 2- and 17-position and thereby relocating the electron density

towards the catalytic centre. In the resulting PMD [(tbbpy)<sub>2</sub>Ru(bmptpphz)PdCl]<sup>2+</sup> (bmptpphz = 2,17-bis(4-methoxyphenyl)tpphz, tbbpy = 4,4'-di-*tert*-butyl-2,2'-bipyridine) the Pd centre coordinated in a tridentate fashion instead of a bidentate one.<sup>[14]</sup> This led to a more stable catalytic unit. Although cyclometalation of the Pd centre led to a higher thermodynamic stability, the catalytic activity was lower.

Similar to bmptpphz, 2,2':6'',2''':6''',2''''-quaterpyridine (qpy) and its derivatives offer a stable multidentate coordination site for metal centres. Qpy in general coordinates in a tetradentate way to a metal centre, forming complexes in *trans* configuration and a highly distorted coordination geometry.<sup>[19]</sup> Currently a large number of qpy complexes have been developed for electro- and photocatalysis, mostly based on abundant transition metals such as cobalt, nickel and iron for H<sub>2</sub> formation and CO<sub>2</sub> reduction and ruthenium and cobalt for water oxidation, which showed remarkable properties regarding stability and catalytic performance.<sup>[19-22]</sup> Despite the apparent capabilities of qpy ligands in stabilising catalytically active metal centres, they can also act as bridging ligands by twisting around their central bond adopting a helical conformation that can bind to two metal centres. In order to restrict this conformational mobility Thummel et al. introduced a phenanthroline motif as backbone.<sup>[23]</sup> On the basis of the dpp (4, 2,9-di(pyridine-2'-yl)-1,10-phenanthroline) ligand they prepared a variety of ruthenium(II) complexes suitable for catalytic water oxidation driven by ceric ammonium nitrate.<sup>[24,25]</sup> Furthermore Wang et al. recently reported a copper(II) based dpp complex, that proved to be an effective water reduction electrocatalyst. Additionally early photocatalytic tests showed potential for future use in photocatalytic systems.<sup>[26]</sup>

Inspired by these works, our aim was to introduce 2-pyridyl substituents in 2- and 17-position of [(tbbpy)<sub>2</sub>Ru(tpphz)]<sup>2+</sup>, thereby creating a ruthenium(II) dye with a modified tpphz ligand that contains a qpy like binding site for a potential second metal centre (Figure 1).

[a] Institute of Inorganic Chemistry I, Ulm University  
Albert-Einstein-Allee 11, 89081 Ulm, Germany  
E-mail: sven.rau@uni-ulm.de  
<http://www.uni-ulm.de/nawi/nawi-anorg1/>

Supporting information for this article is given via a link at the end of the document.

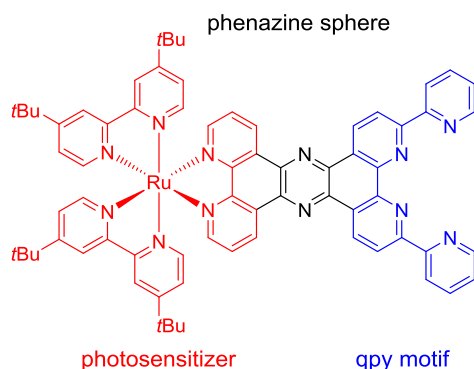


**Figure 1.** Structure of  $[(tbbpy)_2Ru(dptpphz)]^{2+}$  (**7**). The photosensitizing unit (red) and the qpy motif (blue) are highlighted.

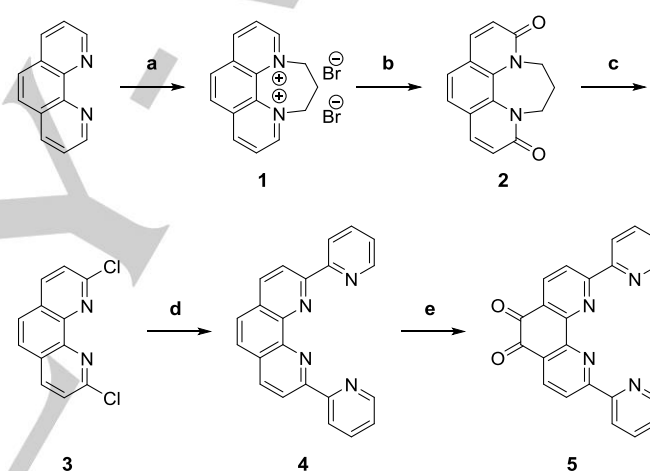
In the present report, we describe the synthesis of  $[(tbbpy)_2Ru(dptpphz)]^{2+}$  (**7**, dptpphz = 2,17-di(pyridin-2-yl)tetrapyrrodo[3,2-a:2',3'-c:3'',2''-h:2''',3''-j]phenazine), its preliminary photophysical and electrochemical characterization, along with concentration dependent dimerization studies.

## Results and Discussion

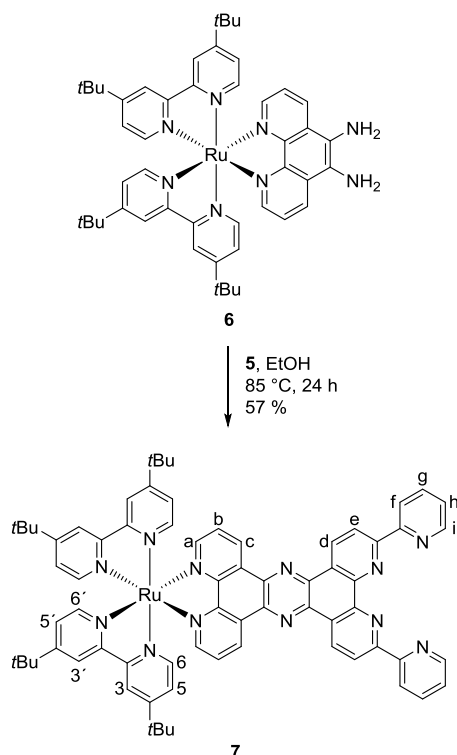
The synthesis of the multidentate ligand **4** was performed using a Pd-mediated Stille cross-coupling reaction between the corresponding phenanthroline and pyridine building blocks. The synthesis route is given in Scheme 1. Chlorinated phenanthroline **3** suitable for Stille reaction was obtained by treatment of the corresponding dione **2** with  $PCl_5$  and  $POCl_3$  following literature known procedures.<sup>[27]</sup> The stannylated pyridine was obtained via a lithium-bromine exchange reaction and consecutive introduction of the stannyl moiety at the 2-position of the pyridine.<sup>[28]</sup> The synthesized precursors 2,9-dichloro-1,10-phenanthroline (**3**) and 2-(tributylstannyl)pyridine were subjected to Stille coupling conditions using tetrakis(triphenylphosphine)palladium(0)  $[Pd(PPh_3)_4]$  as catalyst and dry toluene as solvent in order to obtain ligand **4**. The extended reaction time of 43 h as well as elevated temperatures presumably led to the formation of Pd-colloids making the purification of **4** tedious. Because of the additional purification steps the compound could be obtained in moderate yields of 62 %, which is in agreement with the literature yield range of 62 to 91 %.<sup>[23,24]</sup> The subsequent oxidation of **4** at 5- and 6-position using KBr and a mixture of nitric and sulfuric acid resulted in 2,9-di(pyridine-2'-yl)-1,10-phenanthroline (**5**). In contrast to literature, the yellow precipitate could just be obtained after neutralization with an aqueous  $NaHCO_3$  solution and only in 49 % yield compared to the reported 86 %. All compounds were characterized by  $^1H$ -NMR and **4** additionally by  $^{13}C$ -NMR and high resolution mass spectroscopy. All data were in agreement with literature.<sup>[24]</sup>

Having dione **5** at hand, a condensation reaction was carried out between **5** and 5,6-diamine-1,10-phenanthroline (Scheme 2). In order to enhance solubility and overcome tedious purification

steps, the complexed phenanthroline species **6**<sup>[29]</sup> was used for the condensation reaction. Being aware of the heat and light sensitivity of the diamine complex, the reaction was performed under inert conditions and exclusion of light. It is noteworthy, that dione **5** was used in a twofold excess for this reaction in order to minimize deamination induced condensation reactions between the amine functionalities. Complex **7** could successfully be isolated in a moderate yield of 57 % by size exclusion chromatography. The successful formation of **7** was confirmed by  $^1H$ - and  $^{13}C$ -NMR, as well as by high resolution mass spectrometry (HRMS). The analysis of H,H-COSY experiments (Figure S10) further allowed the assignment of proton signals for the molecule in the aromatic region (Figure 2. and Scheme 2). According to the  $C_2$ -symmetry of the molecule, **7** displays two chemically equivalent molecule sites. Gratifyingly most of the signals are well separated, while just two sets of signals (e- and 3'- as well as h- and 5-signals) overlap with each other.



**Scheme 1.** Synthesis route towards 2,9-di(pyridin-2-yl)-1,10-phenanthroline-5,6-dione (**5**). **a**: 1,3-dibromopropane, nitrobenzene, 120 °C, 5 h, 94 %; **b**:  $K_3[Fe(CN)_6]$ , NaOH,  $H_2O$ , 0 °C, 2 h, 30 %; **c**:  $PCl_5$ ,  $POCl_3$ , 115 °C, 22 h, quantitative; **d**: 2-(tributylstannyl)pyridine,  $[Pd(PPh_3)_4]$ , dry toluene, 115 °C, 43 h, 62 %; **e**: KBr,  $H_2SO_4$ ,  $HNO_3$ , 85 °C, 2 h, 49 %.



**Scheme 2.** Condensation reaction between **5** and **6**. Signal position notation of **7** used in  $^1\text{H-NMR}$  experiments is given in letters and numbers.

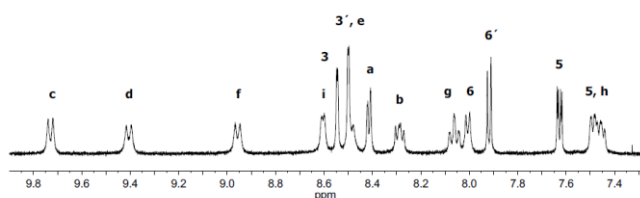


**Figure 2.** Aromatic region of the  $^1\text{H-NMR}$  spectrum of **7** measured in  $\text{CD}_2\text{Cl}_2$  with a complex concentration of 2.95 mM.

To highlight the potential of the tetradentate coordination site of dtpphz, **7** was treated with a  $\text{Zn}^{\text{II}}$  solution in MeCN at room temperature for to coordination at the qpy motif. Since  $\text{Zn}^{\text{II}}$  is known to coordinate to two dpp ligands in a tridentate fashion,<sup>[30]</sup> a 10-fold excess of  $\text{Zn}^{\text{II}}$  was used, to ensure the formation of a dinuclear complex. It is noteworthy, that  $\text{Zn}(\text{BF}_4)_2$  was chosen as the source of  $\text{Zn}^{\text{II}}$  in order to avoid coordinating anions. Gratifyingly, the formation of the Zn complex could be followed by  $^1\text{H-NMR}$  spectroscopy. Measurement of a  $^1\text{H-NMR}$  spectrum after five minutes upon the addition of Zn followed by additional measurements at every eight minutes revealed a completed

formation of the Zn complex within five minutes, evident by the change from a poorly resolved  $^1\text{H-NMR}$  spectrum of **7** in  $\text{CD}_3\text{CN}$  to a well resolved one after the addition of  $\text{Zn}(\text{BF}_4)_2$  solution (Figure S12). However a detailed comparison of the spectra of **7** and **7 + Zn** is troublesome, since the latter produces poorly resolved spectra in  $\text{CD}_2\text{Cl}_2$  (Figure S13). The  $^1\text{H-NMR}$  spectrum in  $\text{CD}_3\text{CN}$  of **7 + Zn** shows 15 sharp signals in the aromatic and two in the aliphatic region which could be assigned by H,H-COSY measurements (Figure S14 and S15). The number of signals indicates  $\text{C}_2$ -symmetry, similar to  $[\text{Zn}(\text{qpy})(\text{OH}_2)_2](\text{BF}_4)_2$  reported by Constable et al.<sup>[31]</sup> Surprisingly, high resolution mass spectrometry gave no additional insight into the structure of the  $\text{Zn}^{\text{II}}$  complex of **7**, since no Zn containing species could be detected.

### Dimerization constant

Molecules exhibiting extended  $\pi$ -conjugation tend to form dimers, a fact that might act detrimental to catalytic activity of the system.<sup>[32]</sup> As such tpphz based complexes have been reported to form dimers due to  $\pi$ - $\pi$ -stacking.<sup>[9,15,32,33]</sup> For this reason the dimerization behaviour of **7** was studied by concentration dependent  $^1\text{H-NMR}$  on the basis of the change of the chemical shift of selected proton signals. Thus  $^1\text{H-NMR}$  spectra were recorded in  $\text{CD}_2\text{Cl}_2$  in a concentration range from 0.23 mM to 39.89 mM, which are shown in Figure 3. Analysis of the spectra revealed that signals attributed to terminal tbbpy ligands underwent only small shifts compared to signals corresponding to the dtpphz ligand. This is not surprising when taking into account that  $\pi$ - $\pi$ -stacking preferably occurs on the dtpphz sphere due to the rigidity of the bridging ligand. Interestingly, all signals that can be ascribed to dtpphz moiety are shifted downfield when increasing the concentration of the complex. The adduct between  $\text{Zn}^{\text{II}}$  and **7** on the other hand did not show any concentration dependent shifts, when varying the concentration (Figure S13). This finding was unsurprising since,  $\text{Zn}^{\text{II}}$  has been used previously to break up  $\pi$ - $\pi$ -stacking tpphz complexes.<sup>[34]</sup>

The concentration dependent shifts can be used to calculate the equilibrium dimerization constant ( $K_D$ ).<sup>[15,33]</sup> For this purpose a set of proton signals was chosen that do not overlap with other signals and subjected to a non-linear least squares global curve fitting approach (see ESI for details). Table 1 summarizes the determined  $K_D$  values for **7** and the reference compounds  $[(\text{tbbpy})_2\text{Ru}(\text{tpphz})]^{2+}$ ,  $[(\text{tbbpy})_2\text{Os}(\text{tpphz})]^{2+}$  and  $[(\text{tbbpy})_2\text{Ru}((\text{tbp})_2\text{tpphz})]^{2+}$  ( $\text{tpphz}(\text{tbp})_2 = 3,16$ -di(tert-butyl-phenyl)-tetrapyrido[3,2-a:2',3'-c:3'',2''-h:2''',3'''-j]phenazine). Compared to  $[(\text{tbbpy})_2\text{Ru}(\text{tpphz})]^{2+}$ , the dimerization constant for **7** is significantly lower (about 70 %).

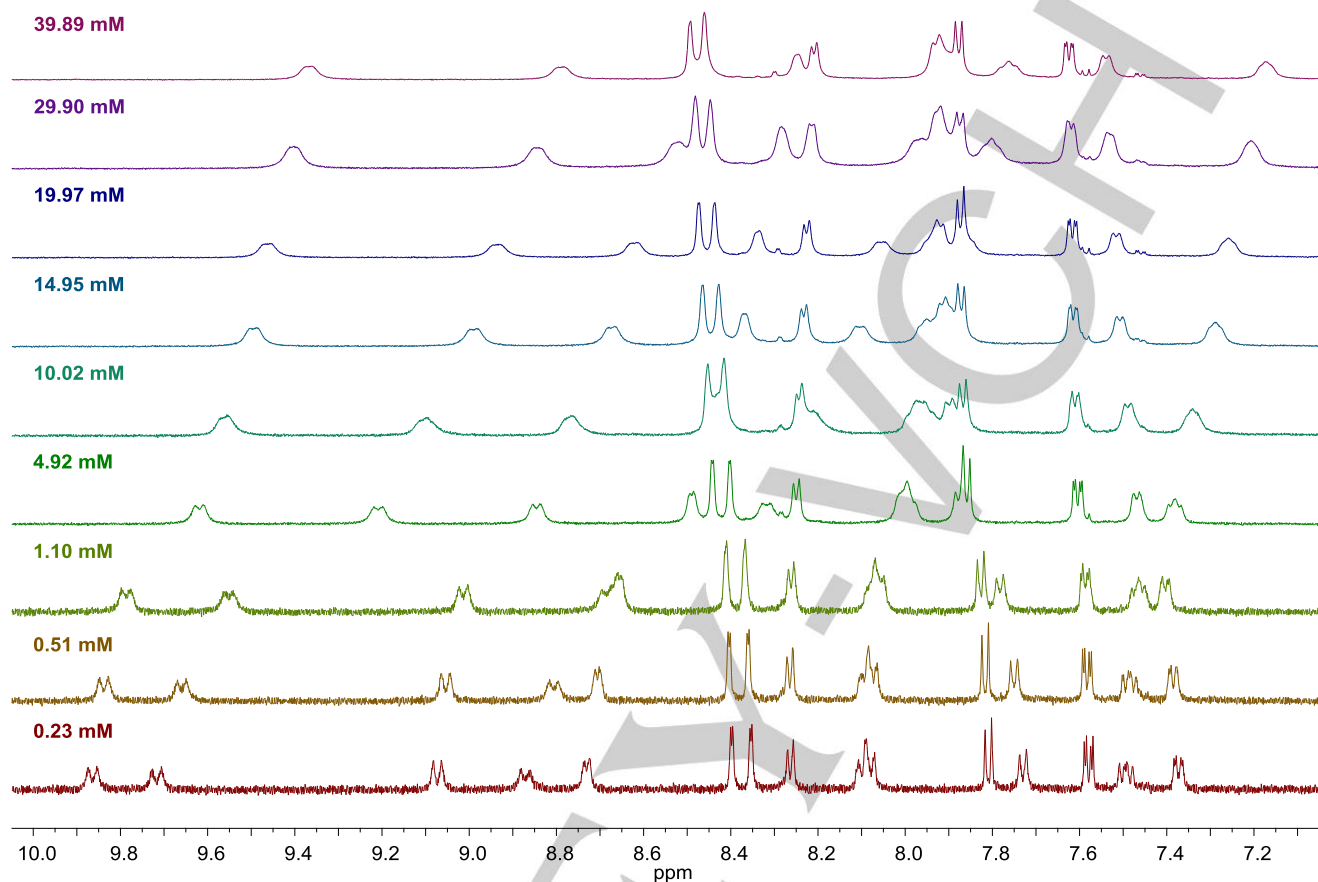


**Figure 3.** Aromatic region of  $^1\text{H-NMR}$  spectra of **7** at different concentrations measured in  $\text{CD}_2\text{Cl}_2$  at room temperature.

This behaviour might result from rotational freedom of pyridyl-groups, inhibiting the planarity along the tpphz sphere. Another possible explanation is steric hindrance between the terminal tbbpy ligands of the ruthenium center and the 2-pyridyl substituents, thereby limiting the possible overlap area of the two  $\pi$ -systems.

### Photophysical properties

The absorption and emission maxima of **7**, **7 + Zn** and  $[(\text{tbbpy})_2\text{Ru}(\text{tpphz})]^{2+}$  as reference compound in  $\text{CH}_2\text{Cl}_2$  and MeCN are summarized in Table 2. The spectra of **7** are depicted in Figure 4. In MeCN a broad absorption in the visible region at 441 nm can be observed. Additionally four absorption bands were detected in the UV region at 288, 335, 377 and at 397 nm. In  $\text{CH}_2\text{Cl}_2$  the absorbance underwent a slight bathochromic shift (4 – 5 nm) with the only exception being the band at 288 nm which did not shift.

**Table 1.** Dimerization constants of **7**,  $[(\text{tbbpy})_2\text{Ru}(\text{tpphz})]^{2+}$ ,  $[(\text{tbbpy})_2\text{Os}(\text{tpphz})]^{2+}$  and  $[(\text{tbbpy})_2\text{Ru}(\text{tpphz}(\text{tpb})_2)]^{2+}$ .

	$K_D$ [ $\text{M}^{-1}$ ]
<b>7</b>	$83 \pm 5$
$[(\text{tbbpy})_2\text{Ru}(\text{tpphz})]^{2+[\text{a}]}$	$289 \pm 17$
$[(\text{tbbpy})_2\text{Os}(\text{tpphz})]^{2+[\text{b}]}$	$400 \pm 40$
$[(\text{tbbpy})_2\text{Ru}(\text{tpphz}(\text{tpb})_2)]^{2+[\text{a}]}$	$647 \pm 46$

[a] Value from ref.<sup>[15]</sup> [b] Value from ref.<sup>[30]</sup>

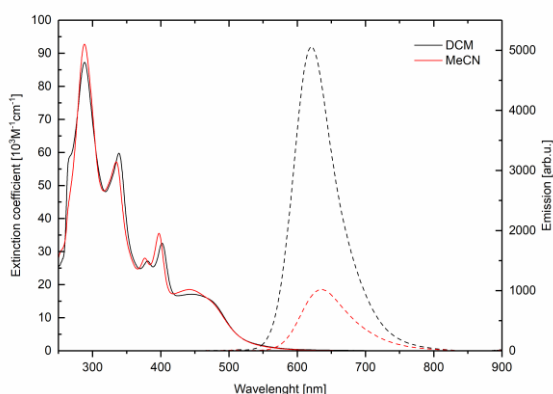


**Figure 4.** UV/vis (solid) and emission (dashed) spectra of **7** in  $\text{CH}_2\text{Cl}_2$  (black) and MeCN (red). Emission spectra were recorded at a complex concentration of  $10^{-4}$  M

**Table 2.** Absorption and emission maxima of **7** in comparison to reference systems and its  $\text{Zn}^{\text{II}}$  adduct.

Compound	Solvent	Absorption $\lambda_{\text{max}}/\text{nm}$ ( $\epsilon/10^3\text{M}^{-1}\text{cm}^{-1}$ )	Emission $\lambda_{\text{max}}/\text{nm}$
<b>7</b>	MeCN	288 (93), 335 (57), 377 (28), 397 (36), 441 (19)	636 <sup>[a]</sup>
	DCM	288 (87), 339 (60), 381 (27), 402 (33), 445 (17)	622 <sup>[b]</sup>
<b>7 + Zn</b>	MeCN	289, sh. <sup>[d]</sup> 323, 337, 367, 388, 444	636 <sup>[a, e]</sup>
	DCM	290, sh. <sup>[d]</sup> 326, 340, sh. <sup>[d]</sup> 367, 389, 448	639 <sup>[b, e]</sup>
[(tbbpy) <sub>2</sub> Ru(tpphz)] <sup>2+</sup> [c]	MeCN	283 (105), sh. <sup>[d]</sup> 314 (45), 379 (31), 442 (20)	633
	DCM	285 (130), sh. <sup>[d]</sup> 315 (46), 382 (26), 444 (19)	620

[a]  $\lambda_{\text{ex}}/\text{MeCN} = 441$  nm. [b]  $\lambda_{\text{ex}}/\text{DCM} = 445$  nm. [c] From ref. <sup>[15]</sup> [d] sh = shoulder. [e] very weak intensity.

Since the absorption spectra of **7** show common features for ruthenium polypyridine complexes with one tpphz based ligand, the nature of the observed bands could be mostly clarified via comparison to [(tbbpy)<sub>2</sub>Ru(tpphz)]<sup>2+</sup> (Figure S18).<sup>[15,16]</sup> The sharp intense absorption around 288 nm can be assigned to  $\pi\text{-}\pi^*$  transitions centred on the tbbpy ligands and the phenanthroline moiety of dptpphz. The bands between 377 and 402 nm correspond to  $\pi\text{-}\pi^*$  transitions on the phenazine sphere. Compared to [(tbbpy)<sub>2</sub>Ru(tpphz)]<sup>2+</sup> this two band structure underwent a redshift of about 17 nm, indicating a stabilizing

effect of the pyridine groups on the excited states of the phenazine motif. This effect was expected due to the electron withdrawing nature of the pyridyl substituents, since similar effects have been reported for tpphz based ruthenium complexes upon introduction of electron withdrawing groups.<sup>[15,16]</sup> Lastly the broad absorption in the visible region around 445 nm can be attributed to the <sup>1</sup>MLCT (metal to ligand charge transfer) from the ruthenium center to the tbbpy ligands and dptpphz. The spectrum of **7** shows an additional absorption band at 335 nm in MeCN and 339 nm in  $\text{CH}_2\text{Cl}_2$ , which is not observable for [(tbbpy)<sub>2</sub>Ru(tpphz)]<sup>2+</sup>. This band likely corresponds to LC (ligand centered) transitions involving the pyridyl substituents. In case of the  $\text{Zn}^{\text{II}}$  adduct two bands related to the phenazine sphere are shifted to lower wavelengths, indicating a destabilizing effect upon coordination of  $\text{Zn}^{\text{II}}$ . Furthermore, the spectral shape of the band assigned to the pyridyl substituents became broader and showed a small shoulder around 323 nm in MeCN and 326 nm in  $\text{CH}_2\text{Cl}_2$ . This change might result from restriction of the rotational freedom of the pyridine groups (Figure S19).

For the measurement of the emission spectra the irradiation wavelength was chosen to match the absorption maximum of the MLCT band in the respective solvent. Complex **7** exhibits an emission at 636 nm in MeCN and at 622 nm in  $\text{CH}_2\text{Cl}_2$ . Measurement in MeCN led to a much lower intensity and a bathochromic shift of 17 nm compared to the spectrum measured in  $\text{CH}_2\text{Cl}_2$ . These findings were unsurprising as MeCN is a more polar solvent and stabilizes the phenazine centered "dark state" due to its higher molecular dipole moment.<sup>[17]</sup> In order to investigate the electronic structure of **7** in more detail, studies towards the water induced light switch effect have been undertaken.<sup>[35]</sup> The extend of this effect was studied by measurement of several emission spectra of **7** in MeCN containing up to 9 v-%  $\text{H}_2\text{O}$ . During this investigation the emission intensity dropped by 47 % in a linear fashion (Figure S20). Likewise literature investigations showed 59-fold decrease in emission quantum yield for [(bpy)<sub>2</sub>Ru(tpphz)]<sup>2+</sup> (bpy = 2,2'-bipyridine), upon measurement of emission spectra in water compared to MeCN.<sup>[36]</sup> The presence of the pronounced water induced light switch effect confirmed the assumption that a so called "dark state" may be populated.<sup>[17,36]</sup> In addition, **7 + Zn** showed only weak emission, independent of the chosen solvent (Figure S21), which is in agreement with investigations of Turro et al., who reported static quenching of the emission of ruthenium tpphz complexes by various transition metals.<sup>[36]</sup> In addition to absorption and emission spectra, excitation spectra were recorded to investigate whether the absorption band related to the pyridine groups contributes to the population of the <sup>3</sup>MLCT state and thereby to its emission (Figure S22). This is apparently the case as the obtained spectra show a maximum at 336 nm in MeCN and at 339 nm in  $\text{CH}_2\text{Cl}_2$  which correspond to the respective absorption spectra.

### Photostability measurements

For ruthenium(II) polypyridyl complexes it is known that they undergo photodecomposition by loss of one of their bipyridine

ligands.<sup>[37–39]</sup> In comparison ruthenium(II) tpphz complexes exhibit a recognizable photostability compared to  $[\text{Ru}(\text{bpy})_3]^{2+}$ , due to the formation of a charge separated excited state located on the tpphz ligand, hampering population of a destabilizing ruthenium centered  $^3\text{MC}$  (metal centered) state.<sup>[40]</sup>

Hence the photostability of **7** was investigated by measuring absorption spectra of a  $10^{-5}$  M complex solution under aerated conditions in MeCN at different times over the course of 22 h. During the experiment the sample was irradiated with blue light (470 nm) by a LED stick (45 – 50  $\text{mW cm}^{-2}$ ) with continuous air cooling (Figure S26). The resulting spectra are depicted in Figure S25.

All absorption bands show a slight decline in intensity. Other than that, the spectral shape remains unchanged upon irradiation, suggesting a fairly high photostability over 22 h for **7**. To put this findings into perspective  $[(\text{tbbpy})_2\text{Ru}(\text{tpphz})]^{2+}$  (Figure S24) and  $[\text{Ru}(\text{bpy})_3]^{2+}$  (Figure S23) were treated the same way as **7** and the time dependent relative decline of their respective MLCT bands was observed and compared to **7** (Figure 5).

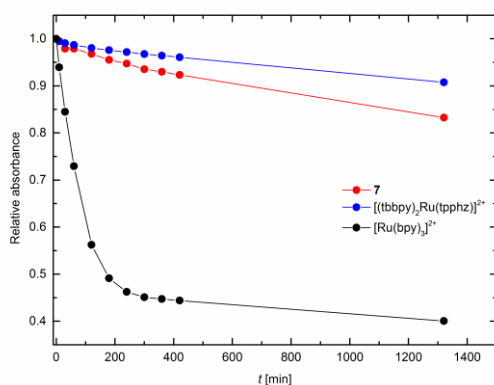


**Figure 5.** Decline of the MLCT absorption band of **7**,  $[\text{Ru}(\text{bpy})_3]^{2+}$  and  $[(\text{tbbpy})_2\text{Ru}(\text{tpphz})]^{2+}$  upon irradiation with blue light of a LED stick ( $\lambda = 470$  nm, 45 – 50  $\text{mW cm}^{-2}$ ).

The MLCT band of **7** drops to 83 % relative to its initial absorption after 22 h, thereby the photostability of **7** is on the same scale as  $[(\text{tbbpy})_2\text{Ru}(\text{tpphz})]^{2+}$  which was slightly more photostable and only drops to 91 %.  $[\text{Ru}(\text{bpy})_3]^{2+}$  on the other hand underwent a relatively fast decomposition and its absorption band dropped to 31 % within 5 h of irradiation and proceeded to drop further to 26 % after 22 h.

This highlights the potential usage of **7** as a dye in supramolecular photocatalysts, since  $[(\text{tbbpy})_2\text{Ru}(\text{tpphz})]^{2+}$  has been reported to enable photocatalytic activity over elongated time periods in such PMDs.<sup>[4,9]</sup>

## Electrochemistry

To gain further insight into the influence of the 2-pyridyl substituents onto the electronic states available in **7**, cyclic voltammetry (CV) measurements were undertaken (Figure 6). The obtained redox halfwave potentials of **7** along with reference compounds are listed in Table 3.

The obtained CV at RT shows a reversible oxidation at +0.80 V assignable to the  $\text{Ru}^{\text{II}}/\text{Ru}^{\text{III}}$  couple, and four ligand based reductions in the studied potential range. For the exact determination of  $E_{\text{red2}} - E_{\text{red4}}$  a CV was measured at 0 °C (Figure S27) due to poor resolution of the respective waves at RT. The reduction processes can be assigned in the following order. The first reduction at -1.40 V is located on the phenazine sphere, the second and third reduction at -1.88 and -2.03 V respectively are assignable to the tbbpy ligands and lastly the second reduction of dtppphz at -2.16 V.<sup>[6,16]</sup> The irreversible shoulder around +0.57 V could not be assigned, however diluting the sample led to a less pronounced shoulder relative to the  $\text{Ru}^{\text{II}}/\text{Ru}^{\text{III}}$  wave, suggesting the irreversible oxidation might result from  $\pi$ - $\pi$ -stacking effects in solution (Figure S28). To get further insight on the nature of this shoulder CV measurements of the  $\text{Zn}^{\text{II}}$  adduct of **7** were performed (Figure 6).

**Table 3.** Electrochemical potentials  $E$  vs.  $\text{Fc}/\text{Fc}^+$  [V] (ferrocene/ferrocenium) for **7** and reference compounds.

	$E_{\text{ox}}$	$E_{\text{red1}}$	$E_{\text{red2}}$	$E_{\text{red3}}$	$E_{\text{red4}}$
<b>7</b>	0.80	-1.40	-1.88	-2.03	-2.16
<b>7</b> + $\text{Zn}^{\text{II}}$	0.86	-1.14	-1.64 <sup>[c]</sup>	-1.87	-2.15
$[(\text{tbbpy})_2\text{Ru}(\text{tpphz})]^{2+[\text{a}]}$	0.83	-1.39	-1.88	-2.05	-2.26
$[(\text{tbbpy})_2\text{Ru}((\text{tpb})_2\text{tpphz})]^{2+[\text{a}]}$	0.86	-1.35	-1.86	-2.02	-2.26
$[(\text{tbbpy})_2\text{Ru}(\text{bmptpphz})]^{2+[\text{b}]}$	0.82	-1.44	-1.90	-2.10	-2.27

[a] From ref. <sup>[15]</sup>. [b] From ref. <sup>[14]</sup>. [c] Estimated value, due to poor resolution.

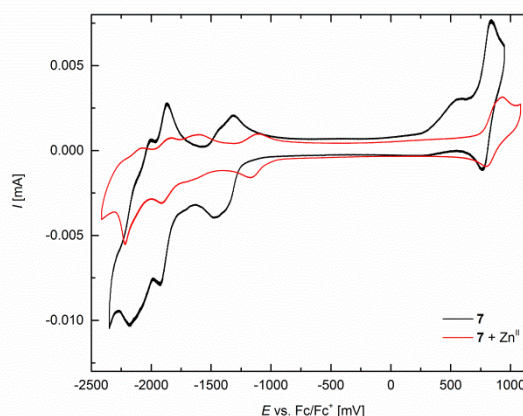


**Figure 6.** Cyclic voltammograms of **7** and **7 + Zn<sup>II</sup>** in MeCN vs. Fc/Fc<sup>+</sup>, containing 0.1 M (*n*Bu)<sub>4</sub>NPF<sub>6</sub> as supporting electrolyte ( $v = 100 \text{ mV s}^{-1}$ ).

The obtained CV of the Zn<sup>II</sup> adduct indeed did not show the previously observed irreversible shoulder of the Ru<sup>II</sup>/Ru<sup>III</sup> wave, further indicating  $\pi$ - $\pi$ -stacking is probably the cause of this shoulder in the CV of **7**. Additionally the oxidation and reduction potentials underwent a shift towards more positive potentials, with the exception of  $E_{\text{red4}}$ .

In comparison to [(tbbpy)<sub>2</sub>Ru(tpphz)]<sup>2+</sup> the second reduction of dptpphz ( $E_{\text{red4}}$ ) ligands proceeds at lower potentials and is shifted to a more positive potential by 0.10 V. At the same time the potentials of the first reductions ( $E_{\text{red1}}$ ,  $E_{\text{red2}}$ ) remain basically unchanged, which suggests that the available electronic states in **7** determining light induced electron transfer processes and population of the excited state located on the phenazine sphere might proceed in a similar manner and timescale like in [(tbbpy)<sub>2</sub>Ru(tpphz)]<sup>2+</sup>.<sup>[10]</sup> Therefore one can also assume that **7** has similar redox requirements for potential catalytic centres.

The shift of  $E_{\text{red4}}$  towards more positive potentials upon the introduction of the 2-pyridine groups may be explainable by their electron withdrawing effect on the tpphz system. Similar effects have been reported for other ruthenium-tpphz complexes that contain electron withdrawing groups.<sup>[15,16]</sup> Likewise negative shifts were reported by Kasuga et al. upon the introduction of electron donating methyl groups.<sup>[18]</sup>

This apparent ease of reduction of the second, qpy-like, coordination sphere might be beneficial for applications of **7** in photocatalytic applications as it could imply a higher driving force for electron transfers.

## Conclusions

The mononuclear ruthenium(II) complex **7** was successfully synthesized via a condensation reaction between the precursor complex **6** and the 5,6-dione of dpp (**5**). Introduction of the 2-pyridyl groups was expected to have a stabilizing effect on the excited states located on the tpphz sphere, which could be confirmed by the observation of bathochromic shift of the phenazine band in the absorption spectrum. Further photostability investigations indicate a similar high stability of **7** compared to [(tbbpy)<sub>2</sub>Ru(tpphz)]<sup>2+</sup>, emphasizing its potential usage as a chromophore in supramolecular photocatalytic systems. Electrochemical investigations revealed that the first two reductions occur at nearly the same potentials as for [(tbbpy)<sub>2</sub>Ru(tpphz)]<sup>2+</sup>, indicating similar redox requirements for possible catalytic centers. At the same time the fourth reduction is shifted towards more positive potentials. Since the introduction of aromatic substituents was expected to promote dimerization, for which tpphz systems are known, concentration dependent <sup>1</sup>H-NMR studies have been conducted to determine the dimerization constant  $K_D$ . Surprisingly **7** showed a significantly lower concentration dependent dimerization, probably due to steric hindrance between the tbbpy ligands and the 2-pyridyl substituents, thereby limiting the possible overlap area of two  $\pi$ -systems.

The complexation of Zn<sup>II</sup> at the newly created tetradentate coordination sphere leads to a loss of stacking behaviour and a significant reduction in emission intensity accompanied by a red shift of the emission wavelength. There is now significant influence on the absorption properties detectable. In addition, irreversible processes in the CV could be inhibited. These results support the assumption that coordination of a metal at the new sphere is possible and that the known ligand properties of the tpphz scaffold are retained.

The present work provides the foundation for the development of new supramolecular photocatalysts.

## Experimental Section

**Materials and Methods.** Commercially available chemicals were used as received. All solvents of technical grade were redistilled through a rotary evaporator prior to use. Solvents of higher quality grade were used without further purification. If not stated otherwise all reactions were carried out under normal laboratory conditions and without the use of absolute solvents. For all reactions carried out under inert conditions standard Schlenk techniques were used with argon as inert gas. 2-(tributylstannyl)pyridine<sup>[28]</sup> [(tbbpy)<sub>2</sub>Ru(tpphz)](PF<sub>6</sub>)<sub>2</sub>,<sup>[4]</sup> **1-3**<sup>[27]</sup> and **4**, **5**<sup>[29]</sup> were prepared according to literature (see ESI for synthetic details). <sup>1</sup>H- and <sup>13</sup>C-NMR spectra were recorded on a Bruker DRX400 with a base frequency of 400 MHz for <sup>1</sup>H- and 101 MHz for <sup>13</sup>C-measurements. The chemical shifts were referred to the signal of the respective deuterated solvent. High resolution mass spectra were measured on a Bruker solariX using electron spray ionization (HRMS/ESI). UV/vis absorption spectra were recorded on a JASCO V-670 and emission spectra on a JASCO FP-8500. In both cases the measurements were performed at room temperature under aerated conditions using HELMA OS precision cells made of quartz glass with a path length of 10 mm. For photostability investigations the samples were irradiated with a LED stick (470 nm, 45 - 50 mW cm<sup>-2</sup>) while being in their respective cells. The cells were cooled during irradiation via a custom made air-cooling apparatus (Figure S19). Cyclic voltammetry (CV) measurements were conducted on a CHI 620E electrochemical workstation, using a standard three electrode configuration with a glassy-carbon electrode (1.6 mm diameter) as working electrode, a Pt-wire as counter electrode and a silver electrode as reference. (*n*-Bu)<sub>4</sub>NPF<sub>6</sub> (0.1 M) was used as supporting electrolyte. Flash-column chromatography was performed on a puriFlash 430 from interchim. Alumina neutral 8 gram flash columns from RediSep R<sub>f</sub> were used as stationary phase.

**Sample preparation for <sup>1</sup>H-NMR dimerization experiments.** Complex **7** was directly weighted out into the NMR tubes, using a concentrated CH<sub>2</sub>Cl<sub>2</sub> stock solution. The solvent was evaporated under slightly elevated temperatures (around 40 °C) and the dry sample was redissolved in 0.5 mL CD<sub>2</sub>Cl<sub>2</sub>. After addition of CD<sub>2</sub>Cl<sub>2</sub> the tubes were sealed with parafilm to prevent loss of the solvent.

**[(tbbpy)<sub>2</sub>Ru(dptpphz)](PF<sub>6</sub>)<sub>2</sub> (**7**).** In a 250 mL Schlenk flask **6** (20.2 mg, 17.8  $\mu\text{mol}$ ) and 13.1 mg **5** (13.1 mg, 35.9  $\mu\text{mol}$ ) were placed and submitted to three vacuum argon cycles and afterwards suspended in dry EtOH (90 mL). The resulting suspension was purged for 95 min with argon before refluxing the mixture under constant stirring for 24 h under argon atmosphere. After the reaction was cooled to room temperature the solvent was evaporated under reduced pressure. The residue was dissolved in a solvent mixture of 47 wt-% chloroform, 30 wt-% acetone and 23 wt-% methanol, and filtrated through a syringe

filter, before purification via a sephadex column (sephadex LH-20). The first red fraction was collected, the solvent removed and the red solid dried under high vacuum to obtain **7** in 57 % (14.8 mg, 10.1  $\mu\text{mol}$ ) yield.  $^1\text{H}$  NMR (400 MHz,  $\text{CD}_2\text{Cl}_2$ ,  $c = 2.95 \cdot 10^{-4}$  M):  $\delta = 9.73$  (d,  $J = 8.0$  Hz, 2H, c-H), 9.41 (d,  $J = 7.9$  Hz, 2H, d-H), 8.96 (d,  $J = 8.0$  Hz, 2H, f-H), 8.60 (d,  $J = 4.0$  Hz, 2H, i-H), 8.55 (d,  $J = 1.7$  Hz, 2H, 3-H), 8.49 (t,  $J = 4.6$  Hz, 4H, 3', e-H), 8.41 (dd,  $J = 5.4$ , 0.9 Hz, 2H, a-H), 8.29 (dd,  $J = 8.1$ , 5.1 Hz, 2H, b-H), 8.06 (td,  $J = 8.0$ , 1.3 Hz, 2H, g-H), 8.01 (d,  $J = 6.5$  Hz, 2H, 6-H), 7.92 (d,  $J = 5.9$  Hz, 2H, 6'-H), 7.63 (dd,  $J = 5.9$ , 2.1 Hz, 2H, 5'-H), 7.47 (ddd,  $J = 12.2$ , 6.1, 2.6 Hz, 4H, 5, h-H), 1.54 (s, 18H, tBu), 1.38 (s, 18H, tBu) ppm.  $^{13}\text{C}$  NMR (101 MHz,  $\text{CD}_2\text{Cl}_2$ ,  $c = 3.99 \cdot 10^{-3}$  M):  $\delta = 163.44$ , 163.41, 158.03, 157.39, 157.28, 155.08, 153.92, 151.84, 151.68, 149.91, 149.38, 147.28, 140.94, 138.83, 137.54, 133.96, 130.27, 128.29, 126.20, 126.18, 126.08, 125.21, 122.27, 121.50, 121.41, 121.16, 120.74 ppm. HRMS/ESI (+): calcd. for  $\text{C}_{70}\text{H}_{66}\text{N}_{12}\text{Ru}$  588.2292, found 588.2292  $[\text{M}-2\text{PF}_6]^{2+}$ , 392.4883  $[\text{M}-2\text{PF}_6+\text{H}]^{3+}$ .

**Zn<sup>II</sup> adduct (7 + Zn<sup>II</sup>).** In a 100 mL flask **7** (15.1 mg, 10  $\mu\text{mol}$ ) was dissolved in a minimal amount of MeCN, to this solution a concentrated  $\text{Zn}(\text{BF}_4)_2$  (24.3 mg, 0.1 mmol) solution in MeCN was added. The resulting mixture was stirred for 4 h at RT. During the course of these 4 h a white precipitate formed, which was filtered off. The remaining red solution was concentrated and the Zn<sup>II</sup> adduct could be obtained via fractional crystallization by diffusing diethyl ether into the solution. The resulting red solid was filtered off and washed with diethyl ether, yielding 63 % (10.7 mg, 6.3  $\mu\text{mol}$ ).  $^1\text{H}$  NMR (400 MHz,  $\text{CD}_3\text{CN}$ ):  $\delta = 10.27$  (d,  $J = 8.6$  Hz, 2H, d-H), 10.03 (dd,  $J = 8.3$ , 1.3 Hz, 2H, c-H), 9.26 (d,  $J = 4.3$  Hz, 2H, i-H), 9.14 (d,  $J = 8.7$  Hz, 2H, e-H), 8.81 (d,  $J = 8.0$  Hz, 2H, f-H), 8.56 (d,  $J = 1.8$  Hz, 2H, 3-H), 8.52 (d,  $J = 1.8$  Hz, 2H, 3'-H), 8.42 (td,  $J = 7.9$ , 1.5 Hz, 2H, g-H), 8.29 (dd,  $J = 5.4$ , 1.3 Hz, 2H, a-H), 8.06 (dd,  $J = 8.2$ , 5.3 Hz, 2H, b-H), 7.99 (ddd,  $J = 7.7$ , 5.2, 0.9 Hz, 2H, h-H), 7.73 (d,  $J = 5.9$  Hz, 2H, 6-H), 7.63 (d,  $J = 6.2$  Hz, 2H, 6'-H), 7.51 (dd,  $J = 6.0$ , 2.0 Hz, 2H, 5-H), 7.25 (dd,  $J = 6.1$ , 2.0 Hz, 2H, 5'-H), 1.47 (s, 18H, tBu), 1.36 (s, 18H, tBu) ppm.

## Acknowledgements

A. M. gratefully acknowledges financial support by a Chemiefonds-Stipendium of Fonds der Chemischen Industrie.

**Keywords:** ruthenium • tetradentate ligands • pi interactions • electrochemistry • photophysics

- [1] B. Gholamkhash, H. Mametsuka, K. Koike, T. Tanabe, M. Furue, O. Ishitani, *Inorg. Chem.* **2005**, *44*, 2326–2336.
- [2] H. Ozawa, M. Haga, K. Sakai, *J. Am. Chem. Soc.* **2006**, *128*, 4926–4927.
- [3] T. A. White, S. L. H. Higgins, S. M. Arachchige, K. J. Brewer, *Angew. Chem., Int. Ed.* **2011**, *50*, 12209–12213.
- [4] S. Rau, B. Schäfer, D. Gleich, E. Anders, M. Rudolph, M. Friedrich, H. Görls, W. Henry, J. G. Vos, *Angew. Chem., Int. Ed.* **2006**, *45*, 6215–6218.
- [5] C. Matlachowski, B. Braun, S. Tschierlei, M. Schwalbe, *Inorg. Chem.* **2015**, *54*, 10351–10360.
- [6] J. Bolger, A. Gourdon, E. Ishow, J.-P. Launay, *Inorg. Chem.* **1996**, *35*, 2937–2944.
- [7] J. Bolger, A. Gourdon, E. Ishow, J.-P. Launay, *J. Chem. Soc. Chem.*

- [8] M. G. Pfeffer, T. Kowacs, M. Wächtler, J. Guthmüller, B. Dietzek, J. G. Vos, S. Rau, *Angew. Chem., Int. Ed.* **2015**, 6627–6631.
- [9] A. K. Mengele, S. Kaufhold, C. Streb, S. Rau, *Dalton Trans.* **2016**, *45*, 6612–6618.
- [10] S. Tschierlei, M. Presselt, C. Kuhnt, A. Yartsev, T. Pascher, V. Sundström, M. Karnahl, M. Schwalbe, B. Schäfer, S. Rau, M. Schmitt, B. Dietzek, J. Popp, *Chem. Eur. J.* **2009**, *15*, 7678–7688.
- [11] C. Chiorboli, M. T. Indelli, F. Scandola, *Top. Curr. Chem.* **2005**, *257*, 63–102.
- [12] C. Chiorboli, C. A. Bignozzi, F. Scandola, E. Ishow, A. Gourdon, J.-P. Launay, *Inorg. Chem.* **1999**, *38*, 2402–2410.
- [13] C. Chiorboli, M. A. J. Rodgers, F. Scandola, *J. Am. Chem. Soc.* **2003**, *125*, 483–491.
- [14] M. G. Pfeffer, L. Zedler, S. Kupfer, M. Paul, M. Schwalbe, K. Peuntinger, D. M. Guldi, J. Guthmüller, J. Popp, S. Gräfe, B. Dietzek, S. Rau, *Dalton Trans.* **2014**, *43*, 11676–11686.
- [15] K. Ritter, C. Pehlken, D. Sorsche, S. Rau, *Dalton Trans.* **2015**, *44*, 8889–8905.
- [16] M. Karnahl, S. Tschierlei, C. Kuhnt, B. Dietzek, M. Schmitt, J. Popp, M. Schwalbe, S. Kriech, H. Görls, F. W. Heinemann, S. Rau, *Dalton Trans.* **2010**, *39*, 2359–70.
- [17] M. Karnahl, C. Kuhnt, F. Ma, A. Yartsev, M. Schmitt, B. Dietzek, S. Rau, J. Popp, *ChemPhysChem* **2011**, *12*, 2101–2109.
- [18] N. Komatsuzaki, R. Katoh, Y. Himeda, H. Sugihara, H. Arakawa, K. Kasuga, *J. Chem. Soc. Dalton Trans* **2000**, 3053–3054.
- [19] Y. Liu, S. M. Ng, S. M. Yiu, W. W. Y. Lam, X. G. Wei, K. C. Lau, T. C. Lau, *Angew. Chem., Int. Ed.* **2014**, *53*, 14468–14471.
- [20] C.-F. Leung, S.-M. Ng, C.-C. Ko, W.-L. Man, J. Wu, L. Chen, T.-C. Lau, *Energy Environ. Sci.* **2012**, *5*, 7903.
- [21] Z. Guo, S. Cheng, C. Cometto, E. Anxolabéhère-Mallart, S. M. Ng, C. C. Ko, G. Liu, L. Chen, M. Robert, T. C. Lau, *J. Am. Chem. Soc.* **2016**, *138*, 9413–9416.
- [22] K. Lam, K.-Y. Wong, S.-M. Yang, C.-M. Che, *J. Chem. Soc. Dalton Trans.* **1995**, 1103–1107.
- [23] R. Zong, R. P. Thummel, *J. Am. Chem. Soc.* **2004**, *126*, 10800–10801.
- [24] G. Zhang, R. Zong, H. W. Tseng, R. P. Thummel, *Inorg. Chem.* **2008**, *47*, 990–998.
- [25] R. Zong, B. Wang, R. P. Thummel, *Inorg. Chem.* **2012**, *51*, 3179–3185.
- [26] Z.-J. Xin, S. Liu, C.-B. Li, Y.-J. Lei, D.-X. Xue, X.-W. Gao, H.-Y. Wang, *Int. J. Hydrogen Energy* **2016**, 1–6.
- [27] J. Frey, T. Kraus, V. Heitz, J. P. Sauvage, *Chem. Eur. J.* **2007**, *13*, 7584–7594.
- [28] C. Braun, E. Spuling, N. B. Heine, M. Cakici, M. Nieger, S. Bräse, *Adv. Synth. Catal.* **2016**, *358*, 1664–1670.
- [29] E. Ishow, A. Gourdon, J.-P. Launay, C. Chiorboli, F. Scandola, *Inorg. Chem.* **1999**, *38*, 1504–1510.
- [30] A. N. Carolan, G. M. Cockrell, N. J. Williams, G. Zhang, D. G. Vanderveer, H. Lee, R. P. Thummel, R. D. Hancock, *Inorg. Chem.* **2013**, *52*, 15–27.
- [31] E. C. Constable, S. M. Elder, M. J. Hannon, A. Martin, P. R. Raithby, D. A. Tocher, *Dalton Trans.* **1996**, 2423–2433.
- [32] M. G. Pfeffer, C. Pehlken, R. Staehle, D. Sorsche, C. Streb, S. Rau, *Dalton Trans.* **2014**, *43*, 13307.
- [33] J. Habermehl, D. Sorsche, P. Murszat, S. Rau, *Eur. J. Inorg. Chem.* **2016**, 3423–3428.
- [34] M. B. Majewski, N. R. De Tacconi, F. M. MacDonnell, M. O. Wolf, *Chem. Eur. J.* **2013**, *19*, 8331–8341.
- [35] A. E. Friedman, J.-C. Chambron, J.-P. Sauvage, N. J. Turro, J. K. Barton, *J. Am. Chem. Soc.* **1990**, *112*, 4960–4962.
- [36] Y. Liu, A. Chouai, N. N. Degtyareva, D. A. Lutterman, K. R. Dunbar, C. Turro, *J. Am. Chem. Soc.* **2005**, *127*, 10796–10797.
- [37] L. Petermann, R. Staehle, M. Pfeifer, C. Reichardt, D. Sorsche, M. Wächtler, J. Popp, B. Dietzek, S. Rau, *Chem. Eur. J.* **2016**, 8240–8253.
- [38] R. F. Jones, D. J. Cole-Hamilton, *Inorg. Chem.* **1981**, *53*, L3–L5.

- [39] P. Vicendo, S. Mouysset, N. Paillous, *Photochem. Photobiol.* **1997**, *65*, 647–655.
- [40] A. Juris, V. Balzani, F. Barigelletti, S. Campagna, P. Belser, A. von Zelewsky, *Coord. Chem. Rev.* **1988**, *84*, 85–277.

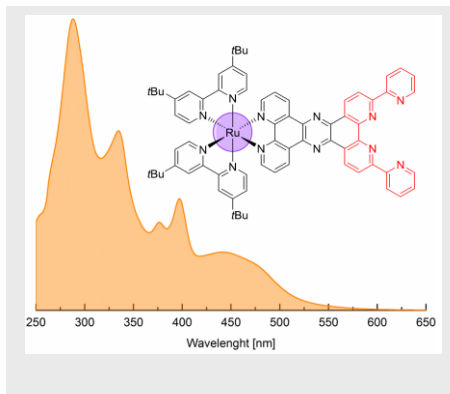
WILEY-VCH

Accepted Manuscript

## Entry for the Table of Contents

## FULL PAPER

The established chromophore  $[(tbbpy)_2Ru(tpphz)]^{2+}$  is modified to contain a tetradentate coordination site and first preliminary photophysical, electrochemical and dimerization studies are undertaken.

**Ruthenium chromophore\***

*Fabian L. Huber, Djawed Nauroozi, Alexander K. Mengele, Sven Rau\**

**Page No. – Page No.**

**Synthesis and characterization of a ruthenium(II) complex for the development of supramolecular photocatalysts containing multidentate coordination spheres**